British Journal of Pharmacology

DOI:10.1111/j.1476-5381.2012.02185.x
www.brjpharmacol.org

RESEARCH PAPER

Benzamil sensitive ion channels contribute to volume regulation in canine chondrocytes

R Lewis[1], CH Feetham[1], L Gentles[1], J Penny[2], L Tregilgas[1], W Tohami[1], A Mobasheri[2] and R Barrett-Jolley[1]

[1]*Musculoskeletal Biology, CIMA, Faculty of Health & Life Sciences, University of Liverpool, Liverpool, UK, and* [2]*Musculoskeletal Research Group, Division of Veterinary Medicine, School of Veterinary Medicine and Science, Faculty of Medicine and Health Sciences, University of Nottingham, Loughborough, UK*

Correspondence
Richard Barrett-Jolley, Musculoskeletal Biology, University of Liverpool, Ageing and Chronic Disease, 4th Floor UCD Building, Daulby Street, Liverpool, Merseyside L69 3GA, UK. E-mail: RBJ@liv.ac.uk

Keywords
chondrocytes; electrophysiology; volume regulation; RVI; resting membrane potential; RMP; ENaC

Received
7 December 2011
Revised
20 July 2012
Accepted
29 July 2012

BACKGROUND AND PURPOSE

Chondrocytes exist within cartilage and serve to maintain the extracellular matrix. It has been postulated that osteoarthritic (OA) chondrocytes lose the ability to regulate their volume, affecting extracellular matrix production. In previous studies, we identified expression of epithelial sodium channels (ENaC) in human chondrocytes, but their function remained unknown. Although ENaC typically has Na^+ transport roles, it is also involved in the cell volume regulation of rat hepatocytes. ENaC is a member of the degenerin (Deg) family, and ENaC/Deg-like channels have a low conductance and high sensitivity to benzamil. In this study, we investigated whether canine chondrocytes express functional ENaC/Deg-like ion channels and, if so, what their function may be.

EXPERIMENTAL APPROACH

Canine chondrocytes were harvested from dogs killed for unassociated welfare reasons. We used immunohistochemistry and patch-clamp electrophysiology to investigate ENaC expression and video microscopy to analyse the effects of pharmacological inhibition of ENaC/Deg on cell volume regulation.

KEY RESULTS

Immunofluorescence showed that canine chondrocytes expressed ENaC protein. Single-channel recordings demonstrated expression of a benzamil-sensitive Na^+ conductance (9 pS), and whole-cell experiments show this to be approximately 1.5 nS per cell with high selectivity for Na^+. Benzamil hyperpolarized chondrocytes by approximately 8 mV with a pD_2 8.4. Chondrocyte regulatory volume decrease (RVI) was inhibited by benzamil (pD_2 7.5) but persisted when extracellular Na^+ ions were replaced by Li^+.

CONCLUSION AND IMPLICATIONS

Our data suggest that benzamil inhibits RVI by reducing the influx of Na^+ ions through ENaC/Deg-like ion channels and present ENaC/Deg as a possible target for pharmacological modulation of chondrocyte volume.

Abbreviations

AQP, aquaporin; Deg, degenerin; ENaC, epithelial sodium channel; OA, osteoarthritis; RMP, resting membrane potential; RVD, regulatory volume decrease; RVI, regulatory volume increase

Introduction

Chondrocytes are the cells of cartilage that synthesize and maintain the substance of cartilage, the extracellular matrix (Stockwell, 1975). They exist in a unique high-pressure, avascular environment, but chondrocytes can be enzymatically isolated from cartilage and largely retain phenotype for the first few passages in culture (Benya and Shaffer, 1982). Recent

studies have shown that chondrocytes, like other cells, express a wide variety of ion channels (Barrett-Jolley *et al.*, 2010) including several species of potassium channel (Wilson *et al.*, 2004; Mobasheri *et al.*, 2005; 2007; 2010; Clark *et al.*, 2010b; 2011) and at least two species of chloride channels (Sugimoto *et al.*, 1996; Tsuga *et al.*, 2002; Funabashi *et al.*, 2010). Our own studies have also shown immunohistologically that human chondrocytes express the epithelial sodium channel (ENaC) (Trujillo *et al.*, 1999). We previously made a preliminary report of their functional expression in canine chondrocytes (Lewis *et al.*, 2008), but their function has been, to date, entirely unknown. ENaC is a low conductance sodium channel consisting of various combinations of three subunits: α, β and γ (Canessa *et al.*, 1994); and our previous immunohistochemical experiments identified each of these in human cartilage (Trujillo *et al.*, 1999). ENaC has the key pharmacological property of sensitivity to low concentrations of benzamil and amiloride and is the prototypic member of the ENaC-degenerin (ENaC/Deg) protein family (Alvarez de la Rosa *et al.*, 2000; Kellenberger and Schild, 2002). The most well characterized function of ENaC is transport of Na^+ across epithelial barriers (Alvarez de la Rosa *et al.*, 2000; Kellenberger and Schild, 2002). As such, ENaC in particular, is a regulator of sodium homeostasis, modulating sodium re-absorption in the kidney (Hager *et al.*, 2001) and sodium absorption from the colon (Kunzelmann and Mall, 2002). However, recent evidence suggests that ENaC has more diverse functions than this, for example, sodium sensing on gustatory neurones of the anterior tongue (Staehler *et al.*, 2008) and neurones in the paraventricular nucleus (Teruyama *et al.*, 2011). ENaC has also been implicated in mechanotransduction in some organisms (discussed by Martinac, 2004; Chalfie, 2009). Specifically, ENaC has been shown to be 'shrink-activated' in certain cell types (Bohmer *et al.*, 2000; Bondarava *et al.*, 2009). Of particular interest to us was the discovery that ENaC has an important (Wehner *et al.*, 2000) and yet complex (Wehner *et al.*, 2006) role in the cell volume regulation of rat hepatocytes. Active volume regulation is a well known physiological response of chondrocytes (reviewed by Lewis *et al.*, 2011b). Under appropriate conditions, they exhibit both regulatory volume decrease (RVD) (Bush and Hall, 2001a,b) and regulatory volume increase (RVI) (Hall *et al.*, 1996; Kerrigan *et al.*, 2006). Typically, in eukaryotic cells, RVI occurs following exposure to hypertonic solutions (Hoffmann *et al.*, 2009). Cells first lose water by osmosis and then shrink; RVI is the process whereby cells recover their volume by accumulating additional solutes and then osmotically imbibing water (Hoffmann *et al.*, 2009). In rat hepatocytes, accumulation of solutes includes influx of sodium ions through ENaC (Wehner *et al.*, 2000; 2006). Furthermore, since ENaC is a relatively sodium selective ion channel (Rossier *et al.*, 1994), one would expect that their activation may lead to membrane depolarization, which could itself have indirect effects on cell function including volume regulation (Lewis *et al.*, 2011a).

In the present study, we sought to characterize both protein and functional expression of ENaC/Deg channels and investigate whether they contribute to the RVI of canine chondrocytes. We show that ENaC is expressed in our canine chondrocyte model, that benzamil sensitive ion channel activity was increased by hypertonic challenge and that these ENaC/Deg-like channels contribute to the RVI response of canine chondrocytes.

Methods

Canine cartilage was obtained from stifle and elbow condyles of skeletally mature, bull terrier-type dogs killed for unrelated clinical reasons. No animals were harmed for this study. Chondrocytes were isolated as described previously (Mobasheri *et al.*, 2010) with type II collagenase. To ensure preservation of the chondrocyte phenotype, we used freshly dissociated and up to third passage cells only.

RVI bioassay

Cells were placed in a 'physiological saline' (Table 1) solution including 145 mM Na^+ and then moved to an identical solution except for the addition of 180 mM sucrose. Cells, at first, shrink as water leaves the cell due to osmosis (Figure 5A phase 'I') and then begin to swell as RVI takes place (Figure 5A phase 'II'). Not all cells showed RVI, and so we used a two 'run' protocol. In the first 'run', we determined if RVI occurred by exposure to hypertonic solution. If this cell did exhibit RVI, we then continued with a second 'run' under either control, or treatment conditions. Live cell imaging was achieved with a Nikon Diaphot microscope equipped with a Sony ICX098QB high-sensitivity CCD, or NIKON Eclipse Ti confocal microscope (Nikon Kingston-Upon-Thames, Surrey, UK). Images were analysed offline with ImageJ (Abramoff *et al.*, 2004). Volume was calculated from the 2D surface area (A) of the cell disc by assuming the cell is approximately spherical as described previously (Walsh and Zhang, 2005; Takeuchi *et al.*, 2006; Lewis *et al.*, 2011a), using the following equation:

$$Vol = \frac{4}{3}\pi\left(\sqrt{\frac{A}{\pi}}\right)^3 \quad (1)$$

Except where stated, data are presented normalized for starting volume (V_0) as V/V_0, where V is the volume at time t. Figure 5A shows confocal images verifying that the chondrocytes were approximately spherical during volume experiments. (Note that the cells only round up when removed from the culture vessels for the duration of the functional experiments, in the immunohistochemistry where they remain on coverslips, they have a flattened appearance). Cells were incubated with FM1-43 dye (Invitrogen, Paisley, UK) before being subjected to the same 'run' treatment as described above.

Electrophysiology

Membrane potentials and whole-cell currents were measured with the whole-cell patch clamp technique using an Axopatch 200A (Molecular Devices, Inc., Sunnyvale, CA), inside-out single channel recordings were made with an Axopatch 200A (Molecular Devices), but cell-attached patch recordings were made with an Axopatch 200B (Molecular Devices, Inc.). Except where stated, data were filtered (1 kHz) using the

inbuilt amplifier filters and sampled (5 kHz) using DigiData 1200 interface cards (Molecular Devices, Inc.). Voltage protocols were run by the WinEDR and WinWCP programs (John Dempster, University of Strathclyde). Osmolarity changes were affected by addition or removal of 180 mM sucrose.

Whole-cell experiments. Patch-pipettes were fabricated from thick-walled borosilicate glass (outer diameter 1.5 mm, inner diameter 0.85 mm) with resistance approximately 5 MΩ when filled. For resting membrane potential (RMP) measurements, we used the standard physiological saline (Table 1), matched with a standard high K^+ 'physiological' intracellular saline solution (Table 2). To measure the sodium permeability of the benzamil-sensitive conductance, a voltage-ramp protocol was used. This consisted of a 4.5 s linear ramp from –80 to +80 mV, repeated at 50 s intervals. Difference currents were obtained by subtraction of a ramp in the presence of benzamil from that run in vehicle control. Intracellular [Na^+] was varied (see Table 2 for the solutions used), and the reversal potential (V_{rev}) of the difference current at each of the $[Na]_i$ used to calculate permeability by fit of a standard variation of the Goldman Hodgkin Katz equation (Equation 2) and minimizing chi^2:

$$V_{rev} = \frac{RT}{F}\ln\left(\frac{[Na]_o + p[K]_o}{[Na]_i + p[K]_i}\right) \quad (2)$$

where $[Na]_o$ is 145 mM, and $[K]_o$ is 5 mM ('ENac Permeability' solution, Table 1). R, T and F have the standard definitions. p is the permeability ratio Na^+/K^+. $[Na]_i$ and $[K]_i$ varied between 22 and 150 mM according to the intracellular solution used (Table 2). Whole-cell currents were also recorded in voltage clamp mode using physiological saline solutions (Tables 1 and 2).

Single channel experiments. Patch pipettes were again fabricated from thick-walled borosilicate 1.5 mm (outer diameter), but resistances were approximately 10 MΩ when filled. For inside-out patch experiments, Na^+ was high in both the patch pipettes (extracellular: 'inside-out patch', Table 1) and the bath (intracellular: 'inside-out patch', Table 2). For single channel kinetics, we used cell-attached patch single channel recording. Sodium ions were replaced by lithium (Li^+) in the patch pipette (extracellular: 'Lithium solution' Table 1) and to nullify the membrane potential, the bath solution (extracellular: 'Cell-attached patch bath solution' Table 1) contained elevated K^+ ions. Since ENaC/Deg channel conductance is so low, it is normal to filter traces heavily before performing kinetic analysis, typical cut-off frequencies from previous studies vary from 50 to 500 Hz (Fyfe and Canessa, 1998; Ishikawa *et al.*, 1998). In our study, we digitally re-filtered the data to 0.5 kHz. Events were then idealized using segmental K means (SKM) methods (Qin, 2004) using QuB software (Dr Feng Qin, Dr Lorin Milescu, Fu Qiong, Chris Nicolai and John Bannen, SUNY, Buffalo, NY). This method alternates between the Viberti method and parameter re-estimation; however, we constrained unitary amplitudes and amplitude distributions to clear periods of openings and closures. Models were fit to the idealized record by optimization of maximum interval likelihood (Qin *et al.*, 1996; 1997). We chose our final model on the basis of significant increases of log-likelihood as described by Lema and Auerbach (2006). The probability density functions (PDFs) drawn in event frequency histogram graphs, and the respective time constants quoted are therefore those calculated *from* the model's fitted rate constants. Where open probability (P_o) was measured from patches with more than one channel, it was calculated as the average of those channels from $Po = I/(Ni)$ where N is number of channels in the patch (estimated as the maximum seen open at one time), and i is the mean unitary amplitude. Conductance was calculated as the slope of the fit of the *IV* curves. Ensemble averages were computed by simply averaging together several raw single channel traces.

The dose–response curve was fit in Sigmaplot (Systat Software, Hounslow, UK) using the following equation, modified from (Black and Shankley, 1985) and (Barrett-Jolley *et al.*, 1999). The SEM values quoted are those calculated by the fitting algorithm.

$$R = m\left(\frac{1-[c]^h}{([c]^h + 10^{-h\cdot pD_2})}\right) \quad (3)$$

R is the response (defined as appropriate in the figure legend), $[c]$ is the concentration of drug, m the maximum value, h is the Hill slope and pD_2 the negative log of the midpoint parameter. Statistical tests were performed using SPSS (SPSS Inc., Chicago, IL), or Minitab (Minitab Ltd, Coventry, UK). Values in text are quoted as mean ± SEM (n), where n is the sample size.

Immunohistochemistry

Primary canine articular chondrocytes were grown in DMEM on autoclaved coverslips at a density of 3×10^5 cells·mL^{-1}. They were then fixed in ice-cold methanol for 10 min, washed and permeabilized with PBS-T and blocked with 10% BSA in PBS. The cells were then incubated with the primary antibodies to the α, β and γ subunits of ENaC (kind gift from Dr Cecilia M Canessa, Yale University, New Haven, CT). These have been used extensively elsewhere (Trujillo *et al.*, 1999; Rubera *et al.*, 2003; Shakibaei and Mobasheri, 2003; Zhang *et al.*, 2005). After three washes with PBS-T, the cells were incubated for 2 h with a goat polyclonal secondary antibody to rabbit IgG (Fc-specific, affinity-purified, pre-adsorbed) conjugated to DyLight® 488 (Abcam, Cambridge, MA, USA; ab98462) diluted according to the manufacturer's recommendations (typically diluted 1:200). After extensive washes in PBS-T, the nuclei were counterstained with propidium iodide (red fluorescence). The chondrocyte surface antigen, CD44, and SOX-9 as an indicator of differentiation, were used as additional controls for chondrocyte phenotype (data not shown). The negative controls were exposed to non-immune rabbit IgG and shows red fluorescent nuclear staining only. The cells were visualized, and digital images were captured using a Leica DM 5000B epifluorescence imaging system.

Software

Software used for each analysis technique is described above, but further details are available at http://pcwww.liv.ac.uk/~rbj/RBJ/software.htm.

Solutions

Table 1

Extracellular solutions used during electrophysiology experiments

Extracellular (mM)	Na	K	Ca	Cl	Mg	Cs	SO_4	$MeSO_4$	Li	Glucose	HEPES	pH 7.4	V_j (mV)
1. Inside-out patch	155	0	4	158	0	0	0	0	0	0	10	NaOH	–5.9
2. Lithium solution	0	9	2	151	1	0	0	0	140	0	10	KOH	–6
3. Cell-attached patch bath solution	0	115	2	122.2	1.6	0	0	0	0	10	10	KOH	
4. Physiological saline	145	5	2	151	1	0	0	0	0	0	10	NaOH	–14.4
5. $NaMeSO_4$	155	0	2	4	0	0	0	150	0	0	10	NaOH	0.5
6. ENaC permeability	158	5	2	159	0	0	0	0	0	0	10	NaOH	[a]

Vj values quoted are when matched with the appropriate intracellular solutions (Table 2). Calculations were performed with JpCalc (Barry and Lynch, 1991). Osmolarity was adjusted in all cases by addition of sucrose as appropriate. Sucrose was chosen to adjust osmolarity so that the ion concentrations remained unchanged during any given experiment. [a]*Vj* varied between 0.1 and 4 mV when paired with intracellular solutions with different sodium concentrations. NB All ion concentrations are the total number of ions in the solution *after* adjustment of pH with NaOH or KOH as appropriate.

Table 2

Intracellular solutions used during electrophysiology experiments

Intracellular (mM)	Na	K	Li	Ca	Cl	Mg	Cs	SO_4	$MeSO_4$	Gluconate	EGTA	BAPTA	TEA	HEPES	pH 7.2
1. Inside-out patch	188	0	0	0	10	0	0	90	0	0	5	0	10	10	NaOH
2. Lithium solution	5	5	140	0	145	0	0	0	0	0	0	0	0	10	NaOH
3. Cell attached patch bath solution[a]															
4. Physiological saline[b]	0	150	0	0	28	1	0	0	0	115	5	0	0	10	KOH
5. $NaMeSO_4$	160	0	0	0	0	0	0	0	150	0	0	5	0	10	NaOH
6. ENaC Permeability	[c]	[c]	0	0	0	0	0	0	0	0	5	0	0	10	NaOH

[a]No intracellular solutions in this configuration. [b]No intracellular solutions were used for the volume recording experiments since cells were intact. [c][Na] and [K] were varied between 22 and 150 mM in these experiments to determine their relative permeability (see Figure 3). All ion concentrations are the total number of ions in the solution *after* adjustment of pH with NaOH or KOH as appropriate.

Results

Functional expression of ENaC/Deg-like channels in canine chondrocytes

We began by showing that our isolated canine chondrocytes expressed positive immunoreactivity for all three subunits of ENaC (α-ENaC, β-ENaC and γ-ENaC; Figure 1A–F). Next, in potassium-free solutions ('Inside-out patch': Tables 1 and 2), we observed a small ion channel in 60% of patches with a slope conductance of 9 ± 1 pS (n = 5) (Figure 1G, I). This reversed near to the equilibrium potential for sodium calculated for these conditions (–4.9 mV) (Figure 1I), and the open probability (*Po*) was significantly reduced by the ENaC/Deg blockers, 10 μM amiloride (Figure 1I) and 100 nM benzamil (inhibition of 96 ± 2%, n = 5 and 56 ± 2%, n = 3, respectively; $P \leq 0.05$ in both cases, ANOVA). The kinetics of this low conductance channel was typical for ENaC channels. To quantify this, we performed a kinetic analysis. Since ENaC channels have an unusually high permeability for Li^+ (Canessa *et al.*, 1994; Schild *et al.*, 1997; Kellenberger *et al.*, 1999), we optimized conditions by recording events under cell-attached patch mode with Li^+ included in the pipette as the charge carrier ('Lithium solution': Table 1). Under this configuration, and with membrane potential of –80 mV, the unitary currents were <1 pA inward, again typical of ENaC/Deg channels. Data was idealized and model fitted as described in the methods. Initially, we found events could not be satisfactorily fitted with a simple two-state model (closed–open) but was much better fitted with two open and two closed states (Figure 2). Best fit rate constants are given in full in Table 3. These rate constants were used to calculate the PDFs, mean open and mean closed times in Figure 2.

We next investigated whether constitutive activity of these channels influenced the cellular membrane potential (V_m). We used standard physiological saline solutions (extracellular: Table 1, intracellular: Table 2) and measured V_m in current clamp mode. Control V_m was –13.2 ± 3.8 mV, similar

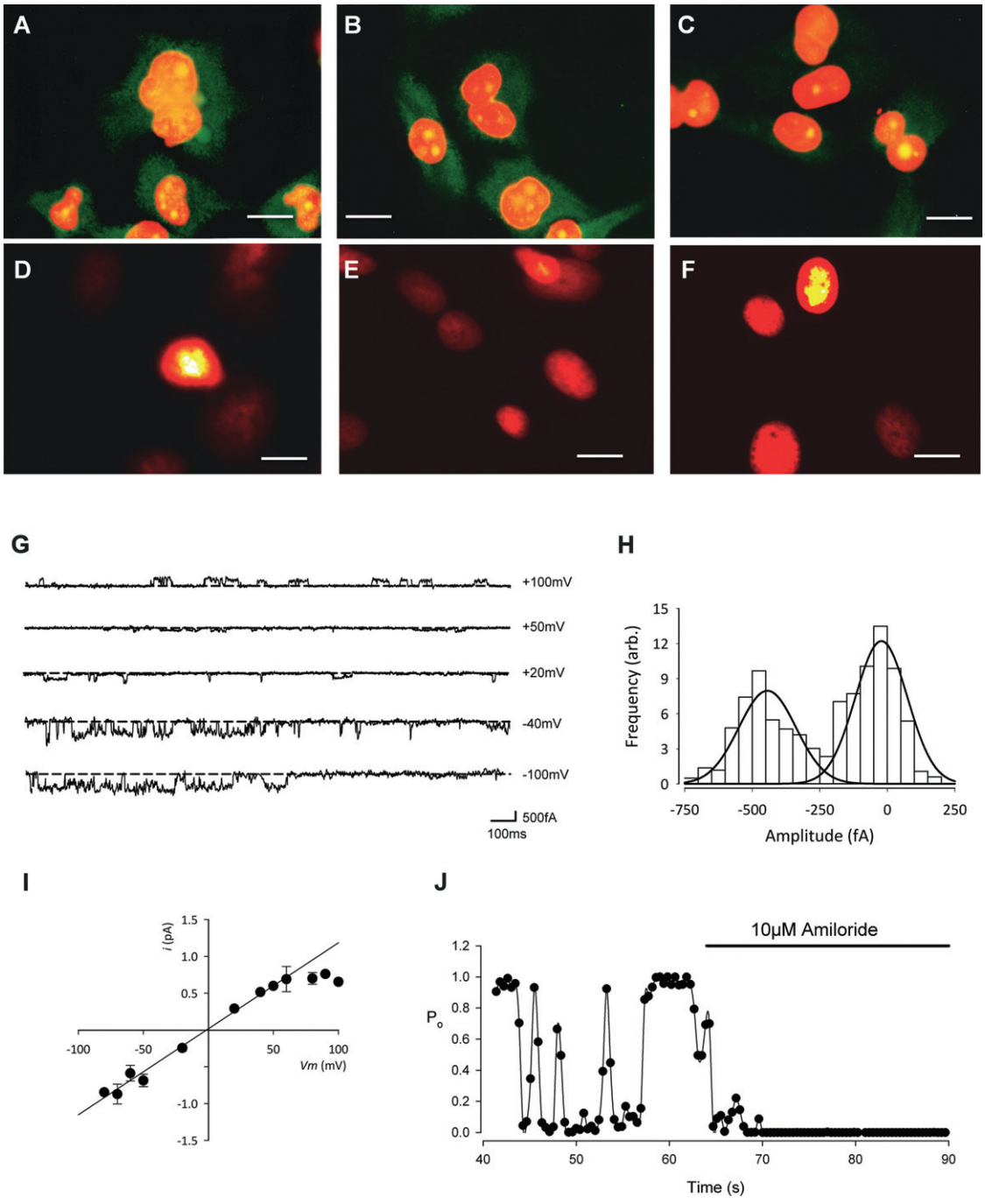

Figure 1

Immunohistochemistry and patch-clamp recording reveal the presence of ENaC protein expression and a benzamil and amiloride sensitive cation conductance. Immunofluorescence staining of αENaC (A), βENaC (B) and γENaC (C) in primary cultures of canine articular chondrocytes (first passage cells, 100× objective). Positive immunoreactivity for all subunits was observed although strongest for α- and β-ENaC. The concentration of the primary antibodies was 1 μg·mL^{-1} (dilution 1:200). The secondary antibody was a goat polyclonal to rabbit IgG (Fc-specific, affinity purified, pre-adsorbed) conjugated to DyLight® 488 (Abcam ab98462). After extensive washes in PBS-T, the nuclei were counterstained with propidium iodide (red fluorescence). Green staining shows the ENaC protein, orange staining is the nuclei and yellow staining is the overlap of the two. (D–F) The negative control was treated identically, but with the omission of primary IgG and shows the red fluorescent nuclear staining with very little background green fluorescence (scale bars for A–F: 10 μm). (G–J) Inside-out patch clamp recordings from canine chondrocytes using inside-out solutions: Tables 1 and 2. (G) Traces of inside-out low conductance single channel activity at the given membrane potentials. The scale bar horizontal line is 100 ms; vertical line is 500 fA. (H) All-points amplitude histogram for the low conductance channel at –40 mV. (I) Single channel current–voltage curve for the low conductance channel. V_{rev} was –1 ± 5 mV (n = 5), slope conductance 9 ± 1 pS (n = 5). (J) Open probability (P_o) versus time, calculated over successive 0.4 s windows before and during the addition of the ENaC channel inhibitor, amiloride (10 μM). Low conductance single channel P_o was reduced by 96 ± 2% (n = 5).

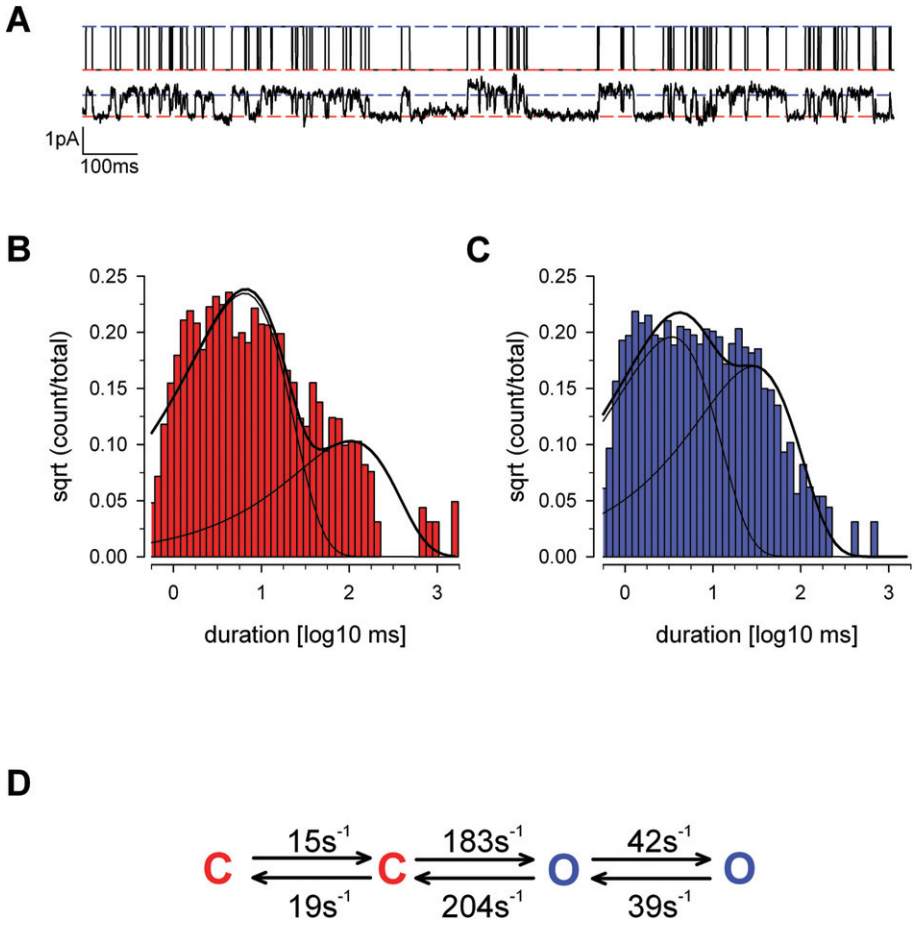

Figure 2

Kinetic analysis of the low conductance cation channel. Kinetic analysis of the ENaC/Deg-like low conductance was performed under cell-attached patch conditions. Li^+ was included in the patch-pipette and served as the charge carrier (Solutions: Table 1). (A) Upper panel, the SKM idealized record from this trace (see Methods). Lower panel, raw single channel trace at –80 mV, baseline corrected. (B) An example patch closed-time distribution superimposed with a bi-exponential PDF calculated from panel D: (τ_1, area): 5.9 ms, 0.83, (τ_2, area): 94.5 ms, 0.17. Mean: 21.0 ms. (C) An example open-time distribution, again fit with a bi-exponential PDF calculated from panel D: (τ_1, area): 3.1 ms, 0.5, (τ_2, area): 26.5 ms, 0.46. Mean: 13.8 ms. (D) Schematic of our best fit kinetic model, full data in text (Table 3). Throughout this figure, red is used to denote closed states, and blue denotes open state.

Table 3

Forward and backward microscopic rate constants for the low conductance channel in 'lithium solution' (Table 1), mean of four experiments

From	To	K (s^{-1})	
State 1	State 2	Mean	SEM
Closed (2)	Open (3)	183.4	21.8
Open (3)	Closed (2)	203.8	5.1
Closed (2)	Closed (1)	19.3	3.0
Closed (1)	Closed (2)	14.6	3.7
Open (3)	Open (4)	41.7	17.0
Open (4)	Open (3)	38.6	9.8

State numbers are in parenthesis (see model in Figure 2).

to previously reported resting membrane potentials in chondrocytes (Wright *et al.*, 1992, Lewis *et al.*, 2011a). Application of 10 μM amiloride caused the V_m to became significantly more negative (Figure 3A, 9.5 ± 0.8 mV, n = 5). Addition of 100 nM benzamil (Figure 3B), an even more specific inhibitor of ENaC (Kellenberger and Schild, 2002; Alexander *et al.*, 2011), also significantly changed V_m (7.5 ± 1.7 mV, n = 5 hyperpolarization, $P \leq 0.05$ ANOVA). These effects were reversible and dose-related (Figure 3A–C).

To determine the sodium permeability of the benzamil-sensitive current (relative to K^+), we switched to whole-cell voltage clamp. With the standard physiological solutions and at a holding potential of –15 mV, application of 1 μM benzamil blocked a small constitutive inward current and resulted in an outward current deflection (mean conductance 1.5 ± 0.4 nS, n = 9, Figure 3). Whole-cell voltage ramps were then run in the presence and absence of benzamil, using four different intracellular sodium concentrations optimized for

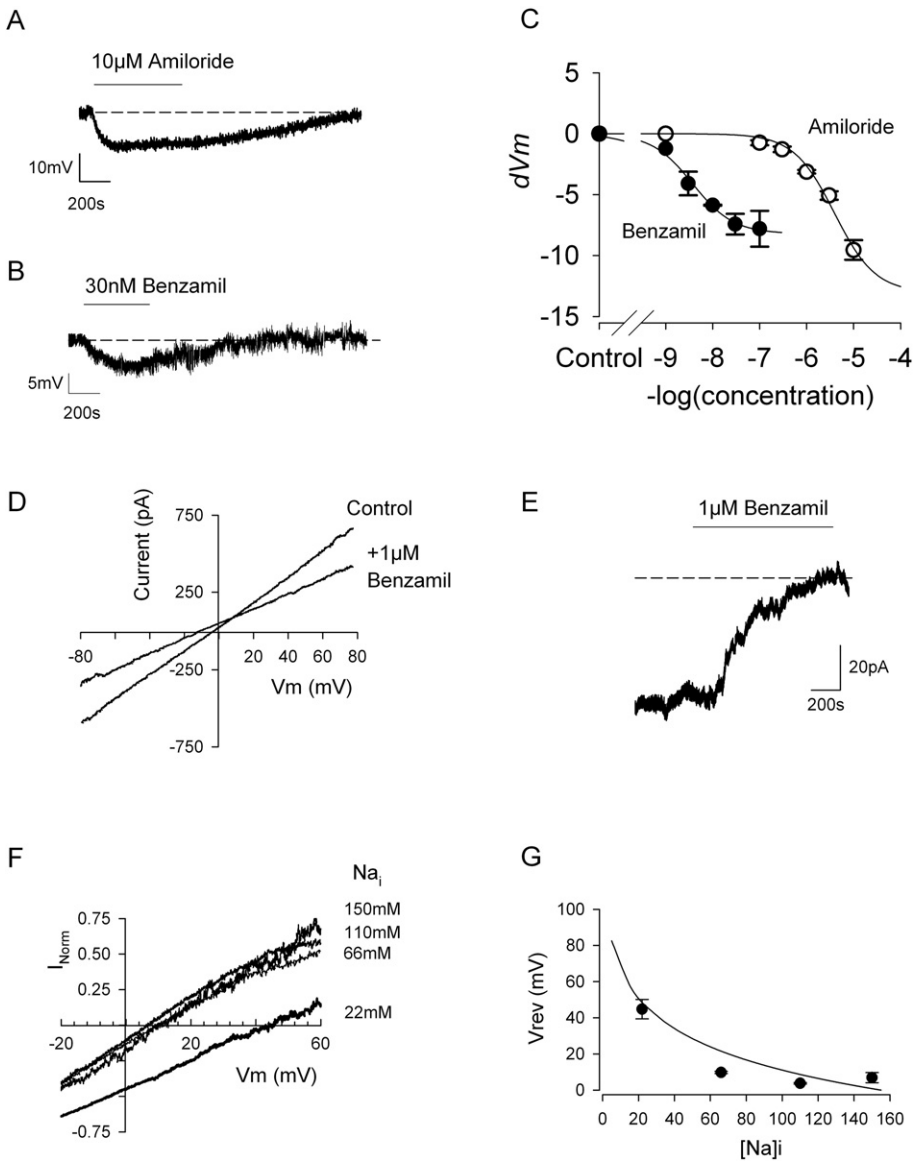

Figure 3

Whole-cell patch clamp shows the presence of a sodium conductance characteristic of ENaC. (A and B) Whole-cell current clamp recordings of a canine chondrocyte in 'physiological saline solutions' (Tables 1 and 2, including 145 mM external NaCl). Application of either amiloride (A) or benzamil (B) reversibly hyperpolarize the membrane. Mean values given in the text. (C) Comparison of the effect of amiloride and benzamil on membrane potential in a number of experiments such as those shown in panels A and B. Data are fitted with Equation 3, where *R* is the change in membrane potential (*dVm*). Hill slope (*h*) was constrained to unity, *m* for amiloride was –13 ± 1.2 mV and pD_2 = 5.5 ± 0.1, for benzamil *m* was –8.2 ± 0.3 mV and pD_2 = 8.4 ± 0.07 (benzamil from eight cells, amiloride each point, three to five cells). (D) Representative whole-cell voltage ramps in 'ENaC permeability' solutions (Tables 1 and 2). The current traces shown illustrate a recording in control and then 1 μM benzamil solution. The resulting difference currents for each combination of solutions is shown in panel F. (E) Representative continuous whole-cell voltage clamp recordings as a chondrocyte is superfused with 1 μM benzamil. The small constitutive inward current is blocked resulting in an increase in outward current corresponding to a mean total whole-cell conductance of 1.5 ± 0.4 nS (*n* = 9). (F) Mean benzamil difference currents with 22 (49), 66 (13), 110 (6) and 150 (7) mM intracellular sodium (calculated Na equilibrium potential in mV) are shown (*n* = 14). (G) Mean V_{rev} plotted against intracellular sodium concentration. The smooth line represents a fit to Equation 2 with *P* (P_{Na}/P_K) of 24.

recording ENaC currents (22, 66, 110 and 150 mM). Subtraction of the whole-cell currents in the presence of benzamil from those recorded in vehicle gave the benzamil difference currents shown in Figure 3F. Difference currents at four different intracellular sodium concentrations were obtained (Figure 3F, G), and the reversal potentials for these followed the calculated changes in Na^+ equilibrium potential (Figure 3G).

Finally, we investigated whether ENaC/Deg channel activity contributed to canine chondrocyte RVI. In cell-attached

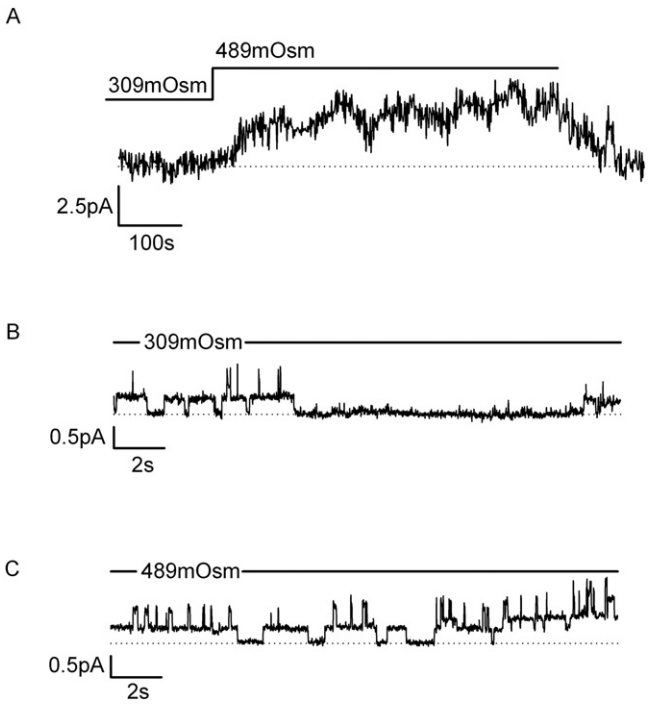

Figure 4

The ENaC/Deg-like channel is activated by exposure to hypertonic solutions. (A) Cells were initially equilibrated in 309mOsm and then switched to 489mOsm as indicated by the bar. Osmolarity was increased with addition of sucrose. An ensemble average of single channel activity is shown (n = 9 patches); the mean increase in current was 4.67 ± 1.7 pA (n = 8, $P \leq 0.05$), and this increase was not seen in the presence of 1 μm benzamil. (B) Representative section taken from one of the 309mOsm records averaged in panel A. (C) Representative section taken from one of the 489mOsm records averaged in panel A.

patch experiments (protocols as above), with Li^+ as the charge carrier ('Lithium solution': Table 1), we found that increasing bath/extracellular osmotic pressure with addition of 180 mM sucrose activated ENaC channels (Figure 4), significantly increasing the open probability of the ENaC/Deg-like channel (from 0.27 ± 0.05 to 0.54 ± 0.07, n = 10, $P \leq 0.05$, paired t-test). In volume recording experiments, we found hypertonic challenge first led to shrinkage, but that within 20 min, volume recovered in approximately 50% of cells. Such volume recovery is termed RVI, and only cells that exhibited RVI under control conditions were used in the following experiments. In cells exhibiting RVI, volume recovered to 92 ± 4%, n = 8 (Figure 5B). The ability of these cells to undergo RVI was maintained when the extracellular Na^+ was completely replaced by Li^+ (Figure 5D), suggesting a Li^+-permeable channel is involved. In Li^+ solutions, cells exhibited slightly less shrinkage; this was still statistically significant shrinkage to 74 ± 3%, $P < 0.001$ and within 20 min of maximum shrinkage returned to 94 ± 2% of starting volume. RVI was inhibited by benzamil with a PD_2 of 7.5 (see Figure 5 for details).

Discussion

In this work, we show that canine chondrocytes express ENaC subunit protein and exhibit single channel activity electrophysiologically and pharmacologically, characteristic of ENaC/Deg channels. Block of these channels significantly alters membrane potential and reduces RVI following osmotic shrinkage.

Identification of ENaC protein and ENaC/Deg-like single channel activity

Several previous studies have demonstrated that isolated chondrocytes exhibit a characteristically differentiated phenotype for the first few passages in culture (Benya and Shaffer, 1982). ENaC protein expression (Trujillo *et al.*, 1999) and RNA transcription (Karlsson *et al.*, 2010) have previously been shown in human chondrocytes. We used reliable and well-tested antibodies that have been used in numerous studies of ENaC (Trujillo *et al.*, 1999; Rubera *et al.*, 2003; Shakibaei and Mobasheri, 2003; Zhang *et al.*, 2005) and found positive immunoreactivity for all three ENaC subunits in canine chondrocytes. Immunostaining did not appear limited to the membrane. There could be several technical reasons for this without need to infer that the majority of protein was cytoplasmic. For immunohistochemical analysis, cells were grown on coverslips and thus morphologically very flat and photographed with epifluorescence (not confocal). These conditions make it difficult to distinguish between membrane and cytoplasmic staining. Second, the standard methods we adopted for fixation/permeabilization vigorously disrupted the membrane with both methanol and detergent. Similar patterns of whole-cell staining have been observed with many membrane ion channels antibodies including those directed against ENaC (Trujillo *et al.*, 1999; Mobasheri *et al.*, 2004; Sauter *et al.*, 2006; Teruyama *et al.*, 2012). Our patch-clamp data show ion channels with physiology and pharmacology consistent with that of ENaC/Deg channels. First, at the single channel level, our measured reversal potential was suggestive of selective Na^+ permeability (Smith and Benos, 1991; Garty and Palmer, 1997), and this was supported by explicit calculation of the permeability ratio P_{Na}/P_K value. In our calculation of permeability ratio, we find that the change in V_{rev} is rather flat at intracellular Na^+ ($[Na]_i$) concentrations between 60 and 150 mM, but V_{rev} rises steeply as $[Na]_i$ falls below 60 mM. This suggests that at the benzamil concentrations used here (1 μM, much greater than our calculated benzamil EC_{50}) there may be a contamination of the ENaC/Deg conductance with a non-specific cation conductance. This would lead to an underestimate of the permeability ratio. Despite this, we calculate a high selectivity for sodium (24:1), very similar to that expected for ENaC (Alexander *et al.*, 2011). Furthermore, these channels had the low conductance that is a key feature of ENaC/Deg channels and ENaC in particular (Kellenberger and Schild, 2002). The value of ENaC single channel conductance depends very much on the subunit composition and the conditions (Kellenberger and Schild, 2002), but our measured value of 9pS lies will within the previously reported range (Canessa *et al.*, 1994; Waldmann *et al.*, 1995; Awayda *et al.*, 1996; Fyfe and Canessa, 1998; Ishikawa *et al.*, 1998; Caldwell *et al.*, 2005). In any set of

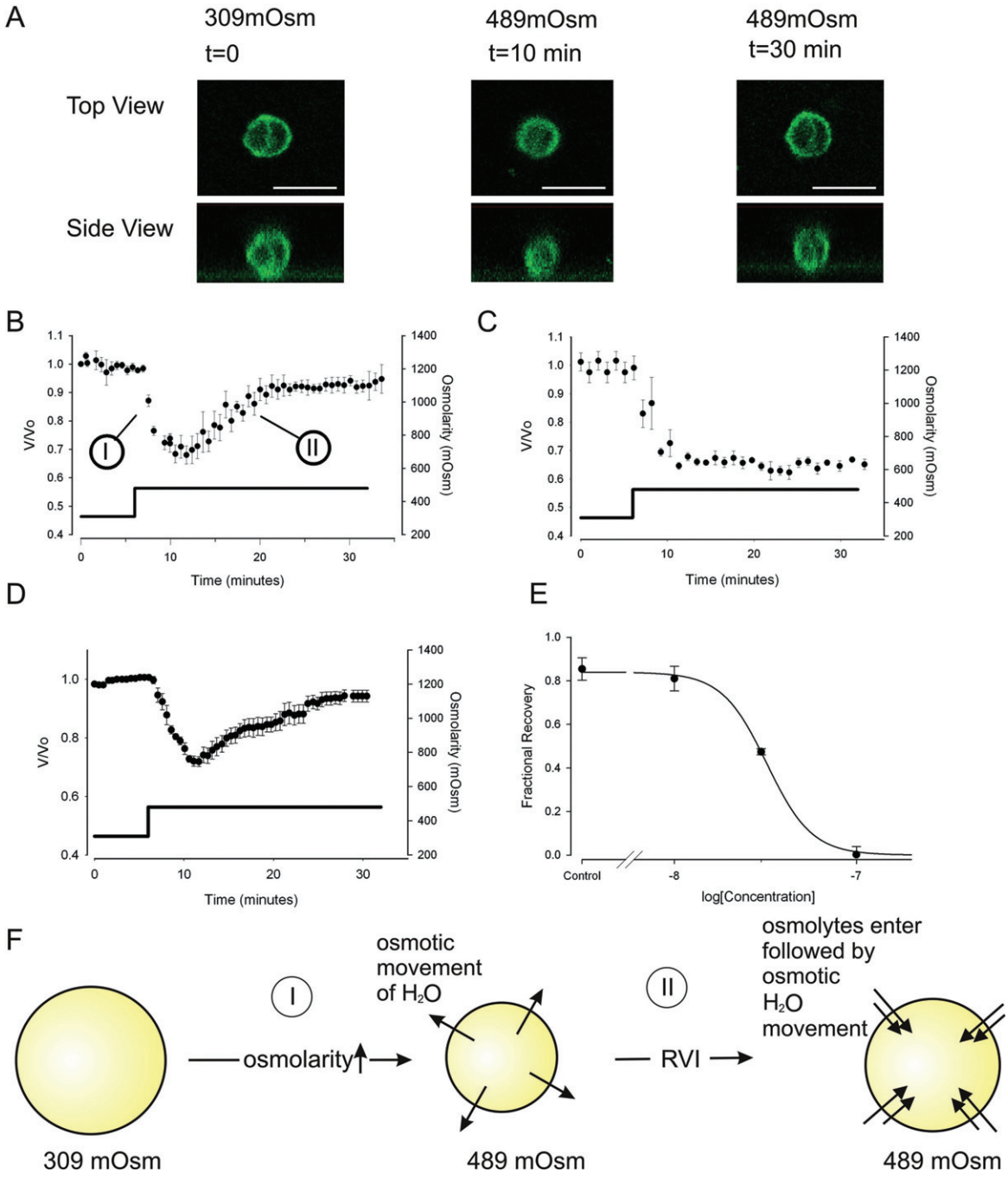

Figure 5

RVI is retained in lithium, but sensitive to low concentrations of benzamil. (A) Confocal images showing changes of cell volume with time. The top panels show the chondrocyte from above (X–Y plane), and the lower panels show the reconstructed cell view from the side (Z–X plane). In order to capture relatively rapid volume changes, scan resolution was set to a low value (31 Z layers per time slice). These images were necessary to verify that cells were approximately spherical (please see Methods: Equation 1). 60× objective scale bar 20 μm. (B) Under control conditions, when cells are incubated in 309mOsm physiological saline (Table 1) then exposed to hypertonic solutions (489mOsm), they first shrink passively as water leaves the cell via osmosis (marked 'I'). They then swell through the process of RVI, eventually returning to the starting volume (RVI indicated by 'II'). Osmolarity was increased with addition of sucrose. Not all cells underwent RVI. We use a two-exposure protocol. Only those cells that exhibited RVI on the first exposure to hypertonic challenge were then used for these experiments. The second exposure either contained benzamil or further control vehicle solution, mean of eight cells. (C) The same protocol as that used in panel B, but with the presence of 100 nM benzamil; RVI is inhibited. Mean of five cells. (D) RVI protocol with extracellular Na^+ replaced by Li^+. For (B) to (D) solid filled markers indicate data points and the solid line (and *y*-axis on the right) indicates the osmolarity. (E) Concentration inhibition curve for inhibition of RVI by benzamil. Five cells per concentration. Data are represented as fractional recovery from the theoretical maximum shrinkage (0.63 = 309/489) and fit with Equation 3, where R is fractional recovery, m was 0.84 ± 0.2, h is 3.5 ± 0.9 and pD_2 =7.5 ± 0.01. (F) Schematic of our working model for RVI, with phases 'I' and 'II' indicated.

electrophysiological experiments on native cells (unlike a recombinant expression system), there is the possibility of mixed populations of channels. In this study, however, the single channel properties, together with the pharmacological profile of these channels (high sensitivity to amiloride and benzamil), are strongly suggestive of the principle component of the low conductance cation channel being ENaC. Acid-sensing channels, specifically ASIC1a (Yuan *et al.*, 2010b), are the only other members of the ENaC/Deg family we are aware of, which have been shown to be present in mammalian chondrocytes. Whilst amiloride (Waldmann *et al.*, 1997; Yuan *et al.*, 2010a) and benzamil (Waldmann *et al.*, 1997) can inhibit these channels at sufficient concentration, benzamil IC_{50} for ASIC1a (Waldmann *et al.*, 1997) is approximately 1000× that of the value we calculated for inhibition of the ENaC/Deg channel in this study (benzamil dV_m EC_{50}, calculated from the fitted pD_2 is equivalent to approximately 4 nM). We found that the inhibition of inside-out patch clamp recorded events were apparently less sensitive to benzamil inhibition than the membrane potential, which would be consistent with an external binding site for ENaC inhibition (Schild *et al.*, 1997). The identity of the low conductance cation channel studied in the present study is therefore highly likely to be ENaC.

The single channel kinetic properties we measured were similar, but not identical, to those of ENaC in other cell types; resting open probability was somewhat lower than reported for ENaC in *Xenopus laevis* oocytes (Fyfe and Canessa, 1998), but similar to that seen in rat cortical collecting tubules (Palmer and Frindt, 1986). Some previous studies found a satisfactory fit with a single open and closed state (Palmer and Frindt, 1986), however, we achieved a much better fit with two open and two closed sates. Palmer and Frindt (1986), for example, saw virtually no short events at all, whereas we saw many. That these differences represent differences in filtering/fitting algorithms is unlikely, but more likely to reflect different subunit expression between systems (Fyfe and Canessa, 1998). Kellenberger *et al.* (2002) used similar filtering conditions to us and also adopted a four-state model to describe their βS518C point mutant ENaC channels. They did not calculate model rate constants, but their mean open and closed states were both considerably shorter than those we observed. The absolute rate constants presented in our schema (Figure 2D) should be viewed with some caution, since single channel kinetic studies with a 9pS channel are likely to be more greatly affected by noise than larger channels. In order to have sufficient signal to noise ratio to perform the study of these very small channels, we had to digitally re-filter the data to 0.5 kHz, rather lower than would usually be desirable for a single channel kinetic analysis study. Whilst the Qin algorithms (Qin, 2004) we used take this into account, it seems logical that the accuracy is less than for a larger channel.

Role of benzamil-sensitive ion channels in volume control

When cells capable of RVI are exposed to hypertonic solutions, three processes take place: first, cells shrink as water leaves the cell along its osmotic gradient; second, the shrinkage in some way activates an influx of ions; and third, water re-enters the cell along this new osmotic gradient until equilibrium is restored (reviewed by Hoffmann *et al.*, 2009). The second and third processes occur in parallel and comprise RVI ('II' in Figure 5A). Whilst the water fluxes are generally accepted to be conducted by aquaporin 'water channels', there is little consensus as to the nature of the shrink-activated influx of ions. It seems likely that it is different from cell type to cell type. ENaC/Deg has previously been shown to be an important component of RVI in rat hepatocytes (Wehner *et al.*, 2000; 2006).

However, despite the importance of volume regulation to chondrocytes, there have been only a few previous studies on RVI in chondrocytes themselves. Activity of the Na^+-K^+-$2Cl^-$-membrane transporter (NKCC) appears to be involved both in chondrocytes (Kerrigan *et al.*, 2006; Bush *et al.*, 2010) and the related C-20/A4 cell line (Qusous *et al.*, 2011), but the Na^+-Ca^{2+} exchanger (NCX) is also implicated, since its block prevents Ca^{2+} ion changes in response to hypertonic challenge (Sanchez and Wilkins, 2004). We certainly do not rule out a contribution of these transporters to volume control, but since benzamil inhibits RVI at well below the concentration required to block NCX, our data are also consistent with a central role for ENaC/Deg. The fact that the EC_{50} for benzamil block of RVI was 3- to 10-fold greater than for block of the ion channel conductance would support a small contribution from a non-ENaC, but benzamil-sensitive conductance. Our working hypothesis is that volume control is a complex process that requires a number of ion channels and transporters to both maintain an appropriate membrane potential and electrochemical gradient to support volume control. Since chondrocytes exhibit both RVD (K^+ efflux) and RVI (Na^+ influx), one would anticipate that optimal RMP would be midway between E_K and E_{Na}. This is consistent with the values we, and others, have found previously (Wright *et al.*, 1992; Lewis *et al.*, 2011a) and in the present study (–13 mV). One would expect E_K for a chondrocyte to be around –80 mV and E_{Na} to be greater than +90 mV (extracellular Na^+ > 200 mM, Urban *et al.*, 1993), thus driving forces for K^+ efflux and Na^+ influx are approximately 70 and 100 mV respectively. Therefore, interestingly, whilst the ENaC/Deg channels have a low conductance, in terms of RVI, there is a huge driving potential for Na^+ influx.

There are therefore at least three ways in which ENaC/Deg block could affect volume regulation: (i) The level of the membrane potential has a strong influence on volume control (Lewis *et al.*, 2011a), and so by hyperpolarizing the cell, ENaC/Deg block could result in a reduced driving force for a hypothetical anionic osmolyte channel. In our experiments, RVI was blocked by 100 nM benzamil, however, which only hyperpolarized the membrane by 8 mV so this would seem unlikely. (ii) ENaC/Deg could be essential for maintaining the electrochemical gradient, and its block could indirectly result in a change such that volume regulation is no longer possible. (iii) ENaC/Deg could open in response to mechanostimulation and allow sufficient Na^+ ion entry to drive RVI. To investigate this possibility, we measured ENaC/Deg channel activity in cell-attached patch mode whilst applying hypertonic saline. Channel activity increased markedly supporting this third alternative mechanism. The mechanism of the opening of ENaC/Deg channels in response to hypertonic solution remains to be determined.

This could again be a direct 'shrink' activation of the channels as previously reported for the ENaC/Deg-like channels in macrophages (Gamper *et al.*, 2000), or the opening in response to a change of intracellular concentration following the cell's response to the hypertonic solutions. Activity of ENaC/Deg is well known to be sensitive to the ionic environment (Anantharam *et al.*, 2006).

Functional significance of volume control in chondrocytes

A number of cell and molecular changes have been shown to take place in cartilage during onset of osteoarthritis (OA). These changes are complex but include changes in proteoglycan content (Venn and Maroudas, 1977; Brocklehurst *et al.*, 1984), loss of collagen (Maroudas, 1976; Venn and Maroudas, 1977), increases in water content (Bollet and Nance, 1966; Mankin and Thrasher, 1975; Brocklehurst *et al.*, 1984; Grushko *et al.*, 1989; Chou *et al.*, 2009) (decreases in osmolarity) and swelling of the chondrocytes themselves (Jones *et al.*, 1999; Bush and Hall, 2003). The sequence of these changes is unknown. However, a decrease in osmolarity does lead to increased vulnerability of chondrocytes to physical damage (Bush *et al.*, 2005). Furthermore, chondrocytes from OA cartilage exhibit poor RVD (Jones *et al.*, 1999), and so it has been suggested that inappropriate increases in chondrocyte volume may contribute to the progression of osteoarthritis (Bush and Hall, 2003). Transgenic deletion of TRPV4, an ion channel critical to volume control in chondrocytes, also predisposes chondrocytes to physical damage (Clark *et al.*, 2010a). Since chondrocytes have robust systems in place to control cellular volume following changes of osmolarity, it seems unlikely that the increase in cellular volume of OA chondrocytes is a simple result of increased cartilage water content. Another possibility is that the changes which take place in cartilage include changes in ion channel expression *per se*. A number of such changes have been reported; a recent transcriptomic analysis showed a total of three ion channels transcript levels increased in chondrocytes from OA cartilage KCNMA1 (large Ca^{2+}-activated potassium channel), KCNN4 (small/intermediated Ca^{2+}-activated potassium channel) and TMEM16A (a Ca^{2+}-activated chloride channel) (Karlsson *et al.*, 2010; Lewis *et al.*, 2011b). They also observed a very significant decrease in the transcript abundance of SCNN1A (ENaC α-subunit) (*ibid*). This observation supports the observation of decreased α-ENaC protein expression previously observed in OA chondrocytes (Trujillo *et al.*, 1999). Whether these changes, or changes in other as yet unidentified ion channels lead to progression of OA, or results from it, remains to be determined. Future studies on models of cartilage degeneration and OA will be necessary to examine whether pharmacological intervention in the processes of chondrocyte volume regulation can influence the progression of OA.

Acknowledgements

RL was funded by the PetPlan Charitable Trust, LG was funded by The Physiological Society.

Conflicts of interest

The authors have no conflicts of interest.

References

Abramoff MD, Magelhaes PJ, Ram SJ (2004). Image processing with ImageJ. Biophotonics Int 11: 36–42.

Alexander SPH, Mathie A, Peters JA (2011). Guide to receptors and channels (GRAC), 5th edition. Br J Pharmacol 164: S1–S324.

Alvarez de la Rosa D, Canessa CM, Fyfe GK, Zhang P (2000). Structure and regulation of amiloride-sensitive sodium channels. Annu Rev Physiol 62: 573–594.

Anantharam A, Tian Y, Palmer LG (2006). Open probability of the epithelial sodium channel is regulated by intracellular sodium. J Physiol 574: 333–347.

Awayda MS, Ismailov II, Berdiev BK, Fuller CM, Benos DJ (1996). Protein kinase regulation of a cloned epithelial Na+ channel. J Gen Physiol 108: 49–65.

Barrett-Jolley R, Dart C, Standen NB (1999). Direct block of native and cloned (Kir2.1) inward rectifier K+ channels by chloroethylclonidine. Br J Pharmacol 128: 760–766.

Barrett-Jolley R, Lewis R, Fallman R, Mobasheri A (2010). The emerging chondrocyte channelome. Front Physiol 1: 135. doi:10.3389/fphys.2010.00135.

Barry PH, Lynch JW (1991). Liquid junction potentials and small cell effects in patch-clamp analysis. J Membr Biol 121: 101–117.

Benya PD, Shaffer JD (1982). Dedifferentiated chondrocytes reexpress the differentiated collagen phenotype when cultured in agarose gels. Cell 30: 215–224.

Black JW, Shankley NP (1985). The isolated stomach preparation of the mouse – a physiological unit for pharmacological analysis. Br J Pharmacol 86: 571–579.

Bohmer C, Wagner CA, Beck S, Moschen I, Melzig J, Werner A *et al.* (2000). The shrinkage-activated Na(+) conductance of rat hepatocytes and its possible correlation to rENaC. Cell Physiol Biochem 10: 187–194.

Bollet AJ, Nance JL (1966). Biochemical findings in normal and osteoarthritic articular cartilage. 2. Chondroitin sulfate concentration and chain length water and ash content. J Clin Invest 45: 1170–1177.

Bondarava M, Li T, Endl E, Wehner F (2009). alpha-ENaC is a functional element of the hypertonicity-induced cation channel in HepG2 cells and it mediates proliferation. Pflugers Arch 458: 675–687.

Brocklehurst R, Bayliss MT, Maroudas A, Coysh HL, Freeman MA, Revell PA *et al.* (1984). The composition of normal and osteoarthritic articular cartilage from human knee joints. With special reference to unicompartmental replacement and osteotomy of the knee. J Bone Joint Surg Am 66: 95–106.

Bush PG, Hall AC (2001a). The osmotic sensitivity of isolated and in situ bovine articular chondrocytes. J Orthop Res 19: 768–778.

Bush PG, Hall AC (2001b). Regulatory volume decrease (RVD) by isolated and in situ bovine articular chondrocytes. J Cell Physiol 187: 304–314.

Bush PG, Hall AC (2003). The volume and morphology of chondrocytes within non-degenerate and degenerate human articular cartilage. Osteoarthritis Cartilage 11: 242–251.

Bush PG, Hodkinson PD, Hamilton GL, Hall AC (2005). Viability and volume of in situ bovine articular chondrocytes – changes following a single impact and effects of medium osmolarity. Osteoarthritis Cartilage 13: 54–65.

Bush PG, Pritchard M, Loqman MY, Damron TA, Hall AC (2010). A key role for membrane transporter NKCC1 in mediating chondrocyte volume increase in the mammalian growth plate. J Bone Miner Res 25: 1594–1603.

Caldwell RA, Boucher RC, Stutts MJ (2005). Neutrophil elastase activates near-silent epithelial Na+ channels and increases airway epithelial Na+ transport. Am J Physiol Lung Cell Mol Physiol 288: L813–L819.

Canessa CM, Schild L, Buell G, Thorens B, Gautschi I, Horisberger JD *et al.* (1994). Amiloride-sensitive epithelial Na+ channel is made of 3 homologous subunits. Nature 367: 463–467.

Chalfie M (2009). Neurosensory mechanotransduction. Nat Rev Mol Cell Biol 10: 44–52.

Chou MC, Tsai PH, Huang GS, Lee HS, Lee CH, Lin MH *et al.* (2009). Correlation between the MR T2 value at 4.7 T and relative water content in articular cartilage in experimental osteoarthritis induced by ACL transection. Osteoarthritis Cartilage 17: 441–447.

Clark AL, Votta BJ, Kumar S, Liedtke W, Guilak F (2010a). Chondroprotective role of the osmotically-sensitive ion channel TRPV4: age- and sex-dependent progression of osteoarthritis in Trpv4 deficient mice. Arthritis Rheum 10: 2973–2983.

Clark RB, Hatano N, Kondo C, Belke DD, Brown BS, Kumar S *et al.* (2010b). Voltage-gated K+ currents in mouse articular chondrocytes regulate membrane potential. Channels 4: 179–191.

Clark RB, Kondo C, Belke DD, Giles WR (2011). Two-pore domain K+ channels regulate membrane potential of isolated human articular chondrocytes. J Physiol 589: 5071–5089.

Funabashi K, Fujii M, Yamamura H, Ohya S, Imaizumi Y (2010). Contribution of chloride channel conductance to the regulation of resting membrane potential in chondrocytes. J Pharmacol Sci 113: 94–99.

Fyfe GK, Canessa CM (1998). Subunit composition determines the single channel kinetics of the epithelial sodium channel. J Gen Physiol 112: 423–432.

Gamper N, Huber SM, Badawi K, Lang F (2000). Cell volume-sensitive sodium channels upregulated by glucocorticoids in U937 macrophages. Pflugers Arch 441: 281–286.

Garty H, Palmer LG (1997). Epithelial sodium channels: function, structure, and regulation. Physiol Rev 77: 359–396.

Grushko G, Schneiderman R, Maroudas A (1989). Some biochemical and biophysical parameters for the study of the pathogenesis of osteoarthritis: a comparison between the processes of ageing and degeneration in human hip cartilage. Connect Tissue Res 19: 149–176.

Hager H, Kwon TH, Vinnikova AK, Masilamani S, Brooks HL, Frokiaer J *et al.* (2001). Immunocytochemical and immunoelectron microscopic localization of alpha-, beta-, and gamma-ENaC in rat kidney. Am J Physiol Renal Physiol 280: F1093–F1106.

Hall AC, Starks I, Shoults CL, Rashidbigi S (1996). Pathways for K+ transport across the bovine articular chondrocyte membrane and their sensitivity to cell volume. Am J Physiol 270: C1300–C1310.

Hoffmann EK, Lambert IH, Pedersen SF (2009). Physiology of cell volume regulation in vertebrates. Physiol Rev 89: 193–277.

Ishikawa T, Marunaka Y, Rotin D (1998). Electrophysiological characterization of the rat epithelial Na+ channel (rENaC) expressed in MDCK cells – Effects of Na+ and Ca2+. J Gen Physiol 111: 825–846.

Jones WR, Ting-Beall HP, Lee GM, Kelley SS, Hochmuth RM, Guilak F (1999). Alterations in the Young's modulus and volumetric properties of chondrocytes isolated from normal and osteoarthritic human cartilage. J Biomech 32: 119–127.

Karlsson C, Dehne T, Lindahl A, Brittberg M, Pruss A, Sittinger M *et al.* (2010). Genome-wide expression profiling reveals new candidate genes associated with osteoarthritis. Osteoarthritis Cartilage 18: 581–592.

Kellenberger S, Schild L (2002). Epithelial sodium channel/degenerin family of ion channels: a variety of functions for a shared structure. Physiol Rev 82: 735–767.

Kellenberger S, Hoffmann-Pochon N, Gautschi I, Schneeberger E, Schild L (1999). On the molecular basis of ion permeation in the epithelial Na+ channel. J Gen Physiol 114: 13–30.

Kellenberger S, Gautschi I, Schild L (2002). An external site controls closing of the epithelial Na+ channel ENaC. J Physiol 543: 413–424.

Kerrigan MJP, Hook CSV, Qusous A, Hall AC (2006). Regulatory volume increase (RVI) by in situ and isolated bovine articular chondrocytes. J Cell Physiol 209: 481–492.

Kunzelmann K, Mall M (2002). Electrolyte transport in the mammalian colon: mechanisms and implications for disease. Physiol Rev 82: 245–289.

Lema GMC, Auerbach A (2006). Modes and models of GABA(A) receptor gating. J Physiol 572: 183–200.

Lewis R, Mobasheri A, Barrett-Jolley R (2008). Electrophysiological identification of epithelial sodium channels in canine articular chondrocytes. Proc Physiol Soc 11: C47.

Lewis R, Asplin K, Bruce G, Dart C, Mobasheri A, Barrett-Jolley R (2011a). The role of the membrane potential in chondrocyte volume regulation. J Cell Physiol 226: 2979–2986.

Lewis R, Feetham C, Barrett-Jolley R (2011b). Cell volume control in chondrocytes. Cell Physiol Biochem 28: 1111–1122.

Mankin HJ, Thrasher AZ (1975). Water-content and binding in normal and osteoarthritic human cartilage. J Bone Joint Surg Am 57: 76–80.

Maroudas A (1976). Balance between swelling pressure and collagen tension in normal and degenerate cartilage. Nature 260: 808–809.

Martinac B (2004). Mechanosensitive ion channels: molecules of mechanotransduction. J Cell Sci 117: 2449–2460.

Mobasheri A, Critchlow K, Clegg RD, Carter SD, Canessa CM (2004). Chronic equine larninitis is characterised by loss of GLUT1, GLUT4 and ENaC positive laminar keratinocytes. Equine Vet J 36: 248–254.

Mobasheri A, Gent TC, Womack MD, Carter SD, Clegg PD, Barrett-Jolley R (2005). Quantitative analysis of voltage-gated potassium currents from primary equine (Equus caballus) and elephant (Loxodonta africana) articular chondrocytes. Am J Physiol 289: R172–R180.

Mobasheri A, Gent TC, Nash AI, Womack MD, Moskaluk CA, Barrett-Jolley R (2007). Evidence for functional ATP-sensitive (K(ATP)) potassium channels in human and equine articular chondrocytes. Osteoarthritis Cartilage 15: 1–8.

Mobasheri A, Lewis R, Maxwell JEJ, Hill C, Womack M, Barrett-Jolley R (2010). Characterization of a stretch-activated potassium channel in chondrocytes. J Cell Physiol 223: 511–518.

Palmer LG, Frindt G (1986). Amiloride-sensitive na channels from the apical membrane of the rat cortical collecting tubule. Proc Natl Acad Sci U S A 83: 2767–2770.

Qin F (2004). Restoration of single-channel currents using the segmental k-means method based on hidden Markov modeling. Biophys J 86: 1488–1501.

Qin F, Auerbach A, Sachs F (1996). Estimating single-channel kinetic parameters from idealized patch-clamp data containing missed events. Biophys J 70: 264–280.

Qin F, Auerbach A, Sachs F (1997). Maximum likelihood estimation of aggregated Markov processes. Proc R Soc Lond B Biol Sci 264: 375–383.

Qusous A, Geewan CSV, Greenwell P, Kerrigan MJP (2011). siRNA-mediated inhibition of Na+ -K+-2Cl(-) cotransporter (NKCC1) and regulatory volume increase in the chondrocyte cell line C-20/A4. J Membr Biol 243: 25–34.

Rossier BC, Canessa CM, Schild L, Horisberger JD (1994). Epithelial sodium channels. Curr Opin Nephrol Hypertens 3: 487–496.

Rubera I, Loffing J, Palmer LG, Frindt G, Fowler-Jaeger N, Sauter D *et al.* (2003). Collecting duct-specific gene inactivation of alphaENaC in the mouse kidney does not impair sodium and potassium balance. J Clin Invest 112: 554–565.

Sanchez JC, Wilkins RJ (2004). Changes in intracellular calcium concentration in response to hypertonicity in bovine articular chondrocytes. Comp Biochem Physiol A Mol Integr Physiol 137: 173–182.

Sauter D, Fernandes S, Goncalves-Mendes N, Boulkroun S, Bankir L, Loffing J *et al.* (2006). Long-term effects of vasopressin on the subcellular localization of ENaC in the renal collecting system. Kidney Int 69: 1024–1032.

Schild L, Schneeberger E, Gautschi I, Firsov D (1997). Identification of amino acid residues in the alpha, beta, and gamma subunits of the epithelial sodium channel (ENaC) involved in amiloride block and ion permeation. J Gen Physiol 109: 15–26.

Shakibaei M, Mobasheri A (2003). Beta1-integrins co-localize with Na, K-ATPase, epithelial sodium channels (ENaC) and voltage activated calcium channels (VACC) in mechanoreceptor complexes of mouse limb-bud chondrocytes. Histol Histopathol 18: 343–351.

Smith PR, Benos DJ (1991). Epithelial Na+ channels. Annu Rev Physiol 53: 509–530.

Staehler F, Riedel K, Demgensky S, Neumann K, Dunkel A, Taeubert A *et al.* (2008). A role of the epithelial sodium channel in human salt taste transduction? Chem Percept 1: 78–90.

Stockwell RA (1975). Chondrocytes. J Anat 119: 395–396.

Sugimoto T, Yoshino M, Nagao M, Ishii S, Yabu H (1996). Voltage-gated ionic channels in cultured rabbit articular chondrocytes. Comp Biochem Physiol C Pharmacol Toxicol Endocrinol 115: 223–232.

Takeuchi A, Tatsumi S, Sarai N, Terashima K, Matsuoka S, Noma A (2006). Ionic mechanisms of cardiac cell swelling induced by blocking Na+/K+ pump as revealed by experiments and simulation. J Gen Physiol 128: 495–507.

Teruyama R, Sakuraba M, Wilson LL, Wandrey NEJ, Armstrong WE (2011). Epithelial sodium channels (ENaC) in magnocellular cells of the rat supraoptic and paraventricular nuclei. Am J Physiol Endocrinol Metab 3: e273–e285.

Teruyama R, Sakuraba M, Wilson LL, Wandrey NEJ, Armstrong WE (2012). Epithelial Na+ sodium channels in magnocellular cells of the rat supraoptic and paraventricular nuclei. Am J Physiol Endocrinol Metab 302: E273–E285.

Trujillo E, Alvarez de la Rosa D, Mobasheri A, Gonzalez T, Canessa CM, Martin-Vasallo P (1999). Sodium transport systems in human chondrocytes. II. Expression of ENaC, Na+/K+/2Cl- cotransporter and Na+/H+ exchangers in healthy and arthritic chondrocytes. Histol Histopathol 14: 1023–1031.

Tsuga K, Tohse N, Yoshino M, Sugimoto T, Yamashita T, Ishii S *et al.* (2002). Chloride conductance determining membrane potential of rabbit articular chondrocytes. J Membr Biol 185: 75–81.

Urban JPG, Hall AC, Gehl KA (1993). Regulation of matrix synthesis rates by the ionic and osmotic environment of articular chondrocytes. J Cell Physiol 154: 262–270.

Venn M, Maroudas A (1977). Chemical composition and swelling of normal and osteoarthrotic femoral-head cartilage .1. chemical composition. Ann Rheum Dis 36: 121–129.

Waldmann R, Champigny G, Bassilana F, Voilley N, Lazdunski M (1995). Molecular cloning and functional expression of a novel amiloride-sensitive Na+ channel. J Biol Chem 270: 27411–27414.

Waldmann R, Champigny G, Bassilana F, Heurteaux C, Lazdunski M (1997). A proton-gated cation channel involved in acid-sensing. Nature 386: 173–177.

Walsh KB, Zhang J (2005). Regulation of cardiac volume-sensitive chloride channel by focal adhesion kinase and Src kinase. Am J Physiol Heart Circ Physiol 289: H2566–H2574.

Wehner F, Bohmer C, Heinzinger H, van den Boom F, Tinel H (2000). The hypertonicity-induced Na+ conductance of rat hepatocytes: physiological significance and molecular correlate. Cell Physiol Biochem 10: 335–340.

Wehner F, Bondarava M, ter Veld F, Endl E, Nurnberger HR, Li T (2006). Hypertonicity-induced cation channels. Acta Physiol 187: 21–25.

Wilson JR, Duncan NA, Giles WR, Clark RB (2004). A voltage-dependent K+ current contributes to membrane potential of acutely isolated canine articular chondrocytes. J Physiol 557: 93–104.

Wright MO, Stockwell RA, Nuki G (1992). Response of plasma-membrane to applied hydrostatic-pressure in chondrocytes and fibroblasts. Connect Tissue Res 28: 49–70.

Yuan F-L, Chen F-H, Lu W-G, Li X, Li J-P, Li C-W *et al.* (2010a). Inhibition of acid-sensing ion channels in articular chondrocytes by amiloride attenuates articular cartilage destruction in rats with adjuvant arthritis. Inflamm Res 59: 939–947.

Yuan F-L, Chen F-H, Lu W-G, Li X, Wu F-R, Li J-P *et al.* (2010b). Acid-sensing ion channel 1a mediates acid-induced increases in intracellular calcium in rat articular chondrocytes. Mol Cell Biochem 340: 153–159.

Zhang YH, Alvarez de la Rosa D, Canessa CM, Hayslett JP (2005). Insulin-induced phosphorylation of ENaC correlates with increased sodium channel function in A6 cells. Am J Physiol Cell Physiol 288: C141–C147.